

CHAPTER 1: INTRODUCTION

For effective skin related treatment and diagnosis with lasers, the decline in laser fluence rate (due to scattering and absorption in the skin) needs to be quantified and compensated for. In the work presented here a simple multi-layer computer model was developed to predict the fluence rate at any pre-determined depth in the skin. The model was validated with experimental measurements on skin simulating phantoms.

Melanin in the epidermal layer of the skin is a major absorber of light in the visible and near infrared region. Due to the lack of data available on the epidermal absorption for different skin phototypes, measurements were done on 30 South African volunteers to establish the expected range of absorption coefficients for the South African population. The reduction in laser fluence rate due to the difference in absorption for the different skin phototypes was evaluated with the multi-layer computer model.

The discipline of biophotonics is an area where sub-fields of physics and biology meet. Biophotonics has become the term for techniques that deal with the interaction between photons and biological media (Vo-Dinh T, 2003) (p1-2). Photons are used to image, detect and manipulate biological materials. The applications of biophotonics allow researchers to see, measure, analyse and manipulate living tissues in ways that have not been possible before for both cellular and bulk tissue (IEEE, 2004), (Peng Q, 2008).

Human skin is considered to be a highly scattering (or turbid) medium for light in the visible and near infrared wavelength regions. Light dosimetry, the study of the irradiation of tissue for treatment purposes, is not yet as well understood as in the case of radiation therapy (Star WM, 1997). The optical properties of human skin and the laser light propagation within skin have been investigated by numerous researchers, (Whitton JT, 1973), (Anderson RR, 1981) (van Gemert MJC, 1989), (Graaff R, 1993), (Jacques S, 2001), (González FJ, 2010), (Doronin A, 2011). These properties are important as they determine the reduction in the laser fluence rate as it propagates through the tissue.

The optimal use of lasers as a treatment modality requires an understanding of the parameters involved in the process. Some of the primary parameters are the penetration depth of the laser light (determined by the optical properties of the tissue), the initial laser power and beam profile. In laser treatment, it is important to determine the fluence rate reaching a certain depth into the organ being treated in order to provide the correct laser irradiance dose (J/cm^2). *In vivo* measurements to determine the fluence rate are seldom

practical. Computer modelling is one of the methods that provide a capability to predict the fluence rate at any given penetration depth into the tissue.

This work focuses on the way that laser light interacts with tissue and the absorption and scattering of the photons as they propagate through the tissue. Photodynamic therapy (PDT) has been used as an application for the computer model developed, to illustrate the effect of the epidermal absorption on the laser transmission through the skin. PDT is a cancer therapy where a photosensitiser (PS) is administered to a patient. The PS accumulates in the tumour and after a period of time the cancerous tumour is irradiated with a laser (Sekkat N, 2012). In order to deliver a therapeutically appropriate amount of laser power to a tumour embedded in the skin, it is important to understand the interaction of laser light with the tissue. In the literature review in Chapter 2, PDT will be discussed in more detail as an example to illustrate the practical application of the work.

The South African population consists of individuals of different ethnicity with a wide range in the skin colours or skin tones. In literature this is referred to as skin type or skin phototype and the standard classification used is the Fitzpatrick skin scale (Fitzpatrick TB, 1988). This scale classifies skin based on its reaction to sun (UV) exposure from skin phototype I (the lightest skin that will always burn due to sun exposure and only turn red and not turn brown) to skin phototype VI (the darkest skin that does not appear to be affected by sun exposure). The range of epidermal absorption coefficients for the different skin phototypes usually present in the South African population is not available in the literature. Measurements were done to determine the absorption coefficient of a small sample of the South African population to establish the typical range of absorption coefficients that may be expected in clinical settings in South Africa. Detailed measurements on a larger sample of the South African population should be conducted but this falls outside the scope of this work.

The continuous increase in medical applications of lasers both for treatment and diagnostic purposes (Peng Q, 2008), (Overton G, 2011) necessitate the ability to model the laser-tissue interaction mechanisms. A computer model was developed to predict the loss of laser light through some tissue layers in order to determine the fluence rate reaching the treatment site. The model was used to predict the fluence rate reaching a tumour 200 μm into the skin for different skin phototypes.

The following objectives were set in this thesis:

1. To develop a computer model that can predict the laser fluence rate some distance into skin.

2. To develop a non-invasive optical measurement technique to determine the epidermal absorption coefficient of an individual.
3. To determine the effect of skin phototype on the absorption of laser light in the epidermis.

The remainder of the thesis is divided into six chapters:

- Chapter 2 - the literature review that addresses the background information required for this work.
- Chapters 3-5 are based on papers published on different aspects of the work. Each chapter consists of a short introduction and information additional to the paper, followed by the paper itself, as published.
 - Chapter 3 - the development of the computer model followed by the paper on the verification of the computer model and validation against optical parameters measured on skin simulating phantoms.
 - Chapter 4 - deals with the determination of the optical properties of human skin. This led to the development and calibration of a diffuse reflectance probe system and software to determine the epidermal absorption coefficient for the different South African skin phototypes. For this work ethics permission was obtained from both the CSIR (Ref 17/2011, Appendix I) and the University of Pretoria (EC110830-060, Appendix II) to do measurements on 30 volunteers.
 - Chapter 5 - the application of the computer model to the various South African skin phototypes. This chapter deals with the effect of both melanin concentration (different skin phototypes) and epidermal thickness on the loss of laser fluence rate through the outer skin layers in PDT treatment for skin cancer.
- Chapter 6 contains the conclusions and possible future work.
- Appendix I and II: Copies of the Ethics approvals.
- Appendix III: Source code of the laser-tissue interaction computer model.

CHAPTER 2: LITERATURE REVIEW

The relevant aspects pertinent as background information will be discussed in this literature review which starts with a discussion of interaction modes of laser light with human tissue and in particular with human skin. Only the relevant skin layers are discussed. This is followed by optical properties applicable to the computer model. Some optical properties were not available in literature. Measurement techniques to determine them are discussed in subsequent sections. A computer model was developed to model the interaction of laser light with human skin. Several light propagation models are discussed briefly before the introduction of the computer model to predict laser fluence rate in the skin. The final section of this chapter provides a very brief summary of an application of the model, which is photodynamic treatment of cancer.

2.1 INTERACTION BETWEEN LASERS AND HUMAN TISSUE

In dealing with the interaction between laser light and human tissue the amount of laser light reaching the target area is of primary importance. The rate of energy delivered per unit area at a specific position is called the fluence rate (W/cm^2) (Welch A, 2011) (p29) and is sometimes referred to as the exposure rate.

It should be noted that all the work in this thesis is based on continuous wave (CW) lasers and that the work concentrates on the macroscopic interaction of light with bulk tissue and does not focus on the cellular interaction.

Laser applications are often portrayed in the popular media as contradictory treatments e.g. enhancing wound healing versus surgical cutting of tissue or as a means of stimulating hair growth versus the removal of unwanted hair. These seemingly conflicting applications of the same technology are possible because of the variety of lasers which are available with a large range of wavelengths, output power or energy and appropriate choices of treatment time (Peng Q, 2008). The interaction of laser light with tissue can be broadly divided into six categories or interaction modes listed in order of increasing treatment times (Peng Q, 2008):

- Electro-mechanical (photochemical or photodisruptive) mode
- Ablation
- Vaporisation
- Coagulation or photothermal processes

- Photochemical (photodynamic) reactions
- Biostimulation and wound healing

The six interaction modes are illustrated in Figures 2.1 and 2.2 (Peng Q, 2008). In Figure 2.2 the fluence rate decreases as a function of increasing interaction time with the tissue and cells. In the high fluence rate applications, the treatment time is very short due to the high intensity of the laser light and the processes are usually destructive/disruptive in nature. For the longer exposure treatments, the fluence rate is much lower to prevent damage to the cells.

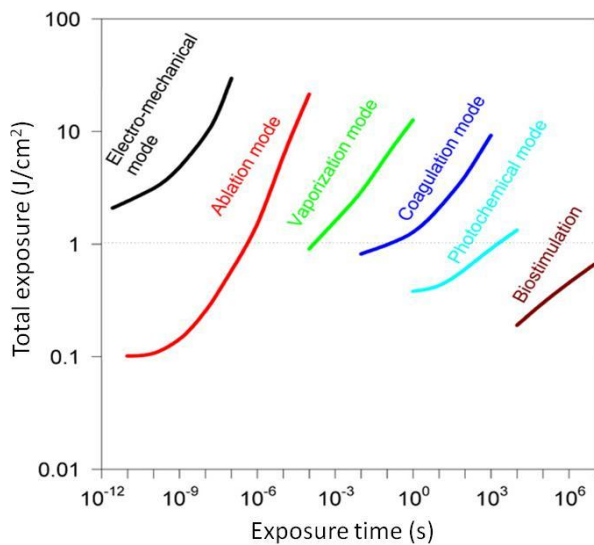


Figure 2.1: Relation between total exposure and exposure time for different modes of laser-tissue interaction (with permission from (Peng Q, 2008)).

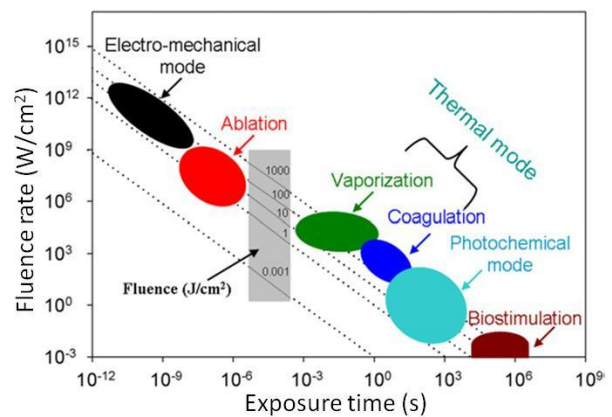


Figure 2.2: Relation between fluence rate and exposure time for different modes of laser-tissue interaction (with permission from (Peng Q, 2008)).

The last two interaction modes, namely photochemical reactions (with PDT as an example) and biostimulation (where penetration into tissue is required), are applicable for this thesis.

2.2 HUMAN SKIN

Human skin is the largest organ of the body, both in terms of volume and surface. The surface area of skin for the average adult is 1.8 m^2 and the weight of the skin is on average 5 kg for males and 4.3 kg for females (Agache P, 2004). The human skin is a complex, heterogeneous medium with blood and pigment spatially distributed in the skin. (Bashkatov AN, 2005).

Skin is generally described as consisting of three main layers (as shown in Figure 2.3):

- The epidermis that is approximately $100 \mu\text{m}$ thick and is blood free.

- The dermis that has blood vessels and is between 1 and 4 mm thick.
- The hypodermis which is a fatty layer consisting of subcutaneous fat and is between 1 and 6 mm thick.

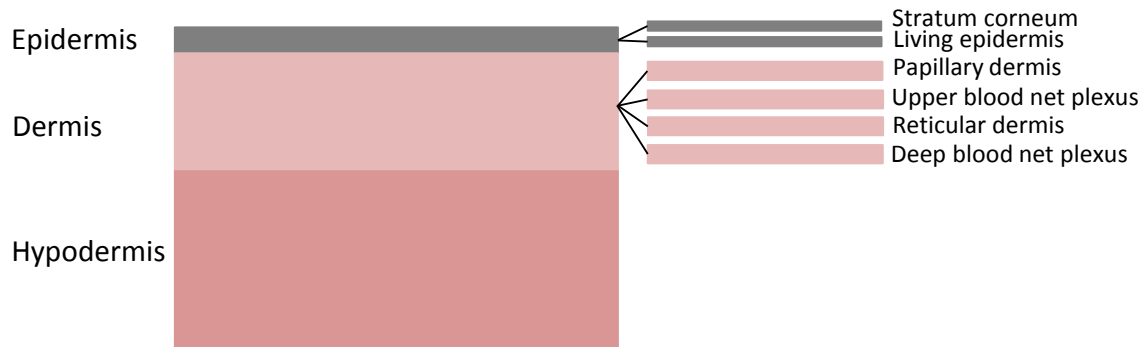


Figure 2.3: Structure of the human skin.

The aim of this thesis is to evaluate the effect of skin phototype on the transmission of light through skin. Only the epidermis has an influence on the skin phototype (see section 2.2.1.2.1 below) and therefore only the epidermis and the next layer, the dermis, will be discussed in more detail.

2.2.1 Epidermis

The epidermis can be divided into two sublayers (Bashkatov AN, 2005), the stratum corneum and the living epidermis.

2.2.1.1 Stratum corneum

The outer layer of the skin is the non-living epidermis, also called the stratum corneum, and is about 10-20 μm thick with a refractive index of 1.55. It consists of dead squamous cells (Bashkatov AN, 2005), (Kollias N, 1995). These cells are highly keratinised with a high lipid and protein content but low water content (Bashkatov AN, 2005).

2.2.1.2 Living epidermis

The second layer is the living epidermis, hereafter referred to as the epidermis. This layer is about 100 μm thick (approximately 10 cell layers) consisting of keratinocytes, melanocytes and Langerhans cells. This layer contains most of the skin pigmentation (i.e. melanin that is produced by the melanocytes) (Kollias N, 1995), (Bashkatov AN, 2005). According to Kollias (Kollias N, 1995) melanin is the major absorbing chromophore in the visible range. The refractive index of the epidermis is close to that of water (nominally 1.33 in the visible

wavelength range), therefore, only weak reflections is expected from the interface between the stratum corneum and the epidermis (Kollias N, 1995). Melanin in the epidermal layer is responsible for the skin colour or skin tone of an individual and impacts on the optical properties of the skin as discussed in section 2.3.

2.2.1.2.1 Melanin

Epidermal melanin can be broadly divided into two families, sulphur poor eumelanin (black-brown colour) and sulphur rich pheomelanin (yellow-reddish colour) (Yoon T, 2003), (Liu Y, 2005), (Costin GE, 2007). Darker coloured skins do not necessarily have more melanocytes than lighter coloured skins, but the melanocytes are more productive and produce more melanin (Störing M, 2004). Melanin in the skin is located in the melanosomes and consists of solid absorbing particles with a diameter between 20 and 40 nm. It is an optically dense material which absorbs light in the visible wavelength region. Melanin is not a single pigment, but consists of various chromophores each with their own optical and physical properties (Alaluf S, 2001). Both eumelanin and pheomelanin are forms of melanin that are synthesized within the melanosomes inside the melanocytes, located in the basal layer (or bottom layer) of the epidermis. The mature melanosomes get transferred via dendrites to the keratinocytes in the epidermis where they are responsible for skin pigmentation and photo-protection (Costin GE, 2007), (Fu D, 2008). A typical 'epidermal unit' consists of one melanocyte that is in contact with about 35-40 neighbouring keratinocytes. It is keratinocytes and fibroblast cells that actively regulate the melanocyte function with respect to cell growth, cell morphology and pigmentation (Yoon T, 2003). The typical extinction coefficients of the eumelanin and pheomelanin as a function of wavelength are shown in Figure 2.4.

The concentration of eumelanin and pheomelanin in an individual depends on both genetic and environmental factors (e.g. sun or UV light exposure). Sun exposed areas yield higher absorption coefficients than areas that are not usually exposed to sunlight.

Eumelanin provides better protection against solar radiation than pheomelanin (Agache P, 2004) (p475). In healthy, photo-exposed skin, the distribution of melanin depends on the exposure of the skin to UVA (315-400 nm) or UVB (290-315 nm) radiation. Exposure to UVB radiation increases the production of melanin and the transfer into keratinocytes. This leads to an increase in the concentration of melanin in the epidermis. UVA exposure increase the melanin in melanocytes and keratinocytes of the basal layer, but the melanin concentration in the rest of the epidermis remains unchanged (Agache P, 2004) (p473-474).

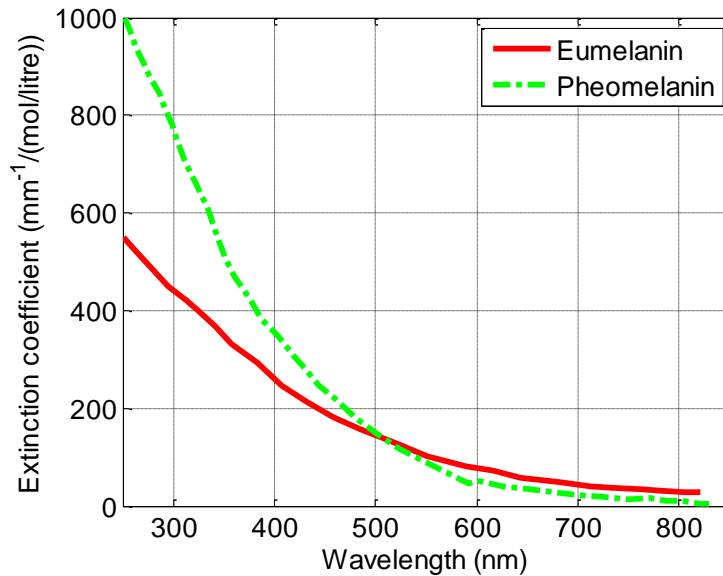


Figure 2.4: Extinction coefficient as a function of wavelength for both of eumelanin and pheomelanin (data from (Jacques S, 2001)).

It is generally believed that one of the major functions of melanin pigmentations is to shield the skin from harmful ultraviolet (UV) radiation (Fu D, 2008). In skin phototypes III to VI (see section 2.2.1.2.2 for the Fitzpatrick scale), the “melanosomes appear to be extensively melanised with solid melanin that has a high molecular weight” (Szabo G, 1969). The refractive index of the melanin is 1.65 (Kurtz SK, 1986), substantially higher than the refractive index of the surrounding medium typically between 1.4 and 1.5, and it is anticipated that the melanin granules may also be strong scatterers of light (Kollias N, 1995) resulting in a higher scattering coefficient. The relationship between melanin and skin absorbance remains a topic of research (Kollias N, 1995), (Alaluf S, 2002(b)), (Lanigan S, 2003), (Lepselter J, 2004), (Liu Y, 2005), (González FJ, 2010).

Even though not all the issues regarding melanin are well understood, it is clear that the melanin concentration impacts on the absorption of laser light in the epidermis and therefore influences the fluence rate available for treatment as will be discussed in Chapters 4 and 5.

2.2.1.2.2 Fitzpatrick skin tone classification

The standard classification for skin tone or skin phototype is the Fitzpatrick skin scale (Fitzpatrick TB, 1988). It is a scale that consists of only six colours to identify the phototype of an individual. This scale classifies skin based on its reaction to sun (UV) exposure and range from skin phototype I (the lightest skin that will always burn due to sun exposure and only turn red and not turn brown) to skin phototype VI (the darkest skin that does not appear

to be affected by sun exposure). A typical Fitzpatrick colour card is shown in Figure 2.5 (Baxamua BN, 2012).

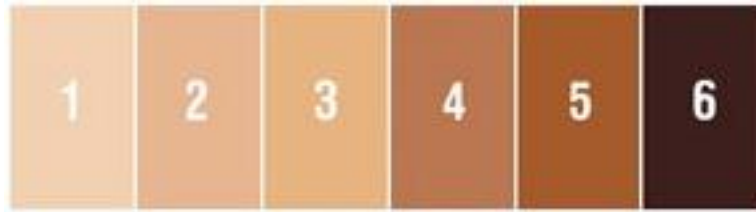


Figure 2.5: Fitzpatrick skin tone colour card.

2.2.2 Dermis

According to Bashkatov (Bashkatov AN, 2005), the dermis can be subdivided into four layers:

- The papillary dermis (150 μm thick).
- The upper blood net plexus (100 μm thick).
- The reticular dermis (1-4 mm thick).
- The deep blood net plexus (100 μm thick).

Even though the dermis can be subdivided into four layers the dermis will be treated as a single layer for the modelling work done later. This is a necessary assumption in order to simplify the model described later in Chapter 3.

The dermis is a vascularised layer with haemoglobin (blood), carotene and bilirubin the main absorbers in the visible region of the light spectrum (Bashkatov AN, 2005). Dermal collagen fibres are the major scatterers of visible light in the dermis, having a refractive index different from that of the surrounding dermis (Scheuplein RJ, 1964), (Kollias N, 1995).

Haemoglobin is the dominant chromophore in the dermis. It exists as either oxyhaemoglobin or deoxyhaemoglobin. In the visible wavelengths, the absorption spectra (Figure 2.6) of both states have characteristic maxima. Haemoglobin is confined to the blood vessels. The perceived redness of the skin is caused by the absorption of light by the haemoglobin in the capillaries and the upper superficial arteriolar and venular plexi. Therefore *ex vivo*, bloodless dermis appears very white (Kollias N, 1995).

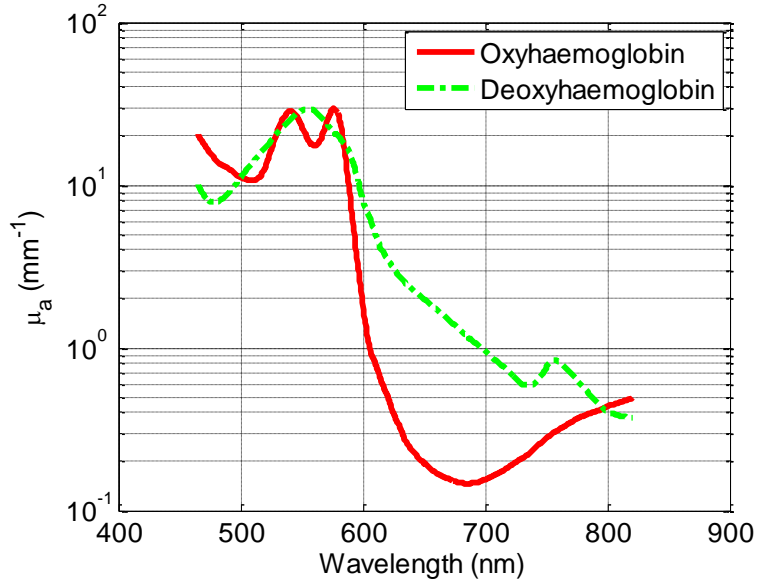


Figure 2.6: Absorption coefficient as a function of wavelength for oxyhaemoglobin and deoxyhaemoglobin (data from (Prahl S, 1999)).

2.3 OPTICAL PROPERTIES

In this section the optical properties of importance for this work will be introduced briefly.

2.3.1 Descriptions and definitions

In discussing the optical properties of tissue it is important to distinguish between the fundamental optical properties and the transport properties used in the modelling work (Jacques S, 2008(b)). The properties of the two groups are listed in Tables 2.1 and 2.2.

Table 2.1: Fundamental optical properties of tissue.

Quantity	Symbol	Units
Refractive index	n	dimensionless
Absorption coefficient	μ_a	cm^{-1}
Scattering coefficient	μ_s	cm^{-1}
Anisotropy of scatter	g	dimensionless

Table 2.2: Transport properties.

Quantity	Symbol	Units
Reduced scattering coefficient	$\mu'_s = (1 - g)\mu_s$	cm^{-1}
Transport mean free path	$MFP' = 1/(\mu_a + \mu'_s)$	cm

For this work it is assumed that the media under investigation are isotropic. This assumption simplifies the description of the fundamental properties without compromising the essential features of the phenomena. Three photo-physical properties are important to describe the propagation of light in biological tissue: refraction, scattering and absorption (Vo-Dinh T, 2003).

2.3.1.1 Refractive index

Refractive index is a fundamental property of homogenous media (Vo-Dinh T, 2003). In a homogeneous medium, the refractive index describes the linear optical properties of the medium. The ratio of the speed of an electromagnetic wave in vacuum to that in a specific medium is known as the absolute refractive index, n , for that medium and is given by (Hecht E, 1974) (p38):

$$n = \frac{c}{v} \quad (2.1)$$

with

c = speed of light in vacuum

v = speed of light in medium

Both the phase speed and the wavelength of the light depend on the refractive index, but the wave frequency and its photon energy ($E = h\nu$) are always the same as in vacuum.

2.3.1.2 Reflection and refraction at an interface

Light propagates in a material/medium until it encounters a boundary with another material (or medium) with a different refractive index. At this point the direction of the light is changed. It will be partially reflected from the surface and refracted when entering the second medium. Snell's law (Eq. 2.2 and Figure 2.7) describes the relation between the incidence angle and the refraction angle (Vo-Dinh T, 2003).

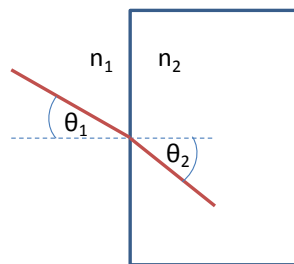


Figure 2.7: Snell's law.

$$n_1 \sin \theta_1 = n_2 \sin \theta_2 \quad (2.2)$$

with

n_1 = refractive index of medium 1

n_2 = refractive index of medium 2

For normal incidence onto a planar boundary, the fraction (T) of the incident energy that is transmitted across the interface is given by:

$$T = \frac{4n_1n_2}{(n_1 + n_2)^2} \quad (2.3)$$

The fraction (R) of the incident energy reflected from the surface (also known as Fresnell reflection) is given by:

$$R = 1 - T = \frac{(n_1 - n_2)^2}{(n_1 + n_2)^2} \quad (2.4)$$

The refractive index of the skin is important due to the changes in refractive index for the different skin layers. Mismatch of the refractive index at the surface of the tissue gives rise to specular reflection of the incident beam (Wilson BC, 1990). The photons that are specularly reflected do not enter the tissue to ‘probe’ the tissue but only provide information regarding the surface roughness and refractive index of the tissue (skin) (Wilson BC, 1990). Diffuse reflected photons that entered the skin provide information regarding the sub-surface skin layers as applied in the diffuse reflectance probe measurements discussed in Chapter 4.

2.3.1.3 Absorption

The major absorbing chromophores in skin are the blood, melanin and water. The absorption coefficient, μ_a , of a medium containing many chromophores with a volume density, ρ_a , and an effective cross-sectional area, σ_a , is defined as (Jacques SL, 1998(a)), (Dam JS, 2000(b)):

$$\mu_a = \rho_a \sigma_a \quad (2.5)$$

[cm⁻¹] [cm⁻³] [cm²]

The measurement unit of μ_a usually used is cm⁻¹, which is not an SI unit but quite practical. The probability of ‘survival’ of a photon (T_p) after a path length, d , (or the transmission of a photon for a distance d) is given by (Jacques SL, 1998(a)):

$$T_p = e^{-\mu_a d} \quad (2.6)$$

This expression is true regardless of whether the photon path is a straight line (ballistic photon) or if the photon was scattered numerous times in an optically turbid medium.

When a photon is detected at a specific position in the skin (or skin surface) it is not possible to determine which path the photon took to the end point. It could have moved to the position with one or two scattering events or in numerous scattering events. This is the so-called similarity principle and is illustrated later in Figure 2.10 in section 2.3.1.6.

Figure 2.8 shows the wavelength dependence of some of the major biological absorbers. The best penetration in skin is for wavelengths where the blood and melanin absorption are a

minimum and the absorption due to the water is still low. This gave rise to the term ‘optical and diagnostic window’ for the wavelength band between 600 and 1000 nm.

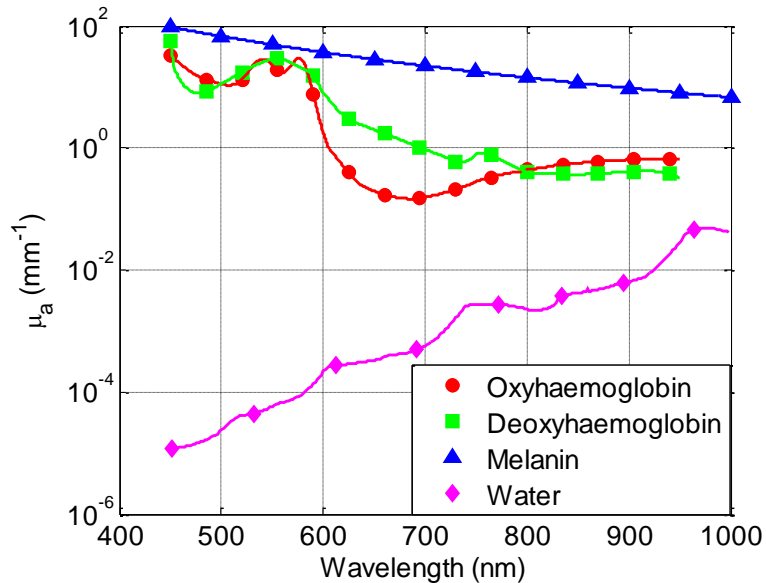


Figure 2.8: Wavelength dependence of the major biological absorbers (from tabulated data (Jacques SL, 1998(a)), (Prahl S, 1999)).

The Beer-Lambert law relates the transmission of light through a medium with the optical properties of the medium and can be written as:

$$I = I_0 e^{-\mu_a d} \quad (2.7)$$

with:

I = measured laser intensity after the sample

I_0 = initial laser intensity

d = optical path length through the medium

μ_a = absorption coefficient

2.3.1.4 Scattering

In biomedical optics, scattering processes are very important in both diagnostic and therapeutic applications. Scattering depends on the size, morphology and structure of the components in tissue (Vo-Dinh T, 2003). Mie theory describes the scattering of light by structures that are of the same size as the wavelength of the photon. Rayleigh scattering describes the scattering of light by structures that are much smaller than the photon wavelength. Figure 2.9 illustrates Mie and Rayleigh scattering of visible and infrared light by tissue structures. Most laser treatments are done in the visible and near infrared part of the light spectrum where the sub-cellular components scatter the light.

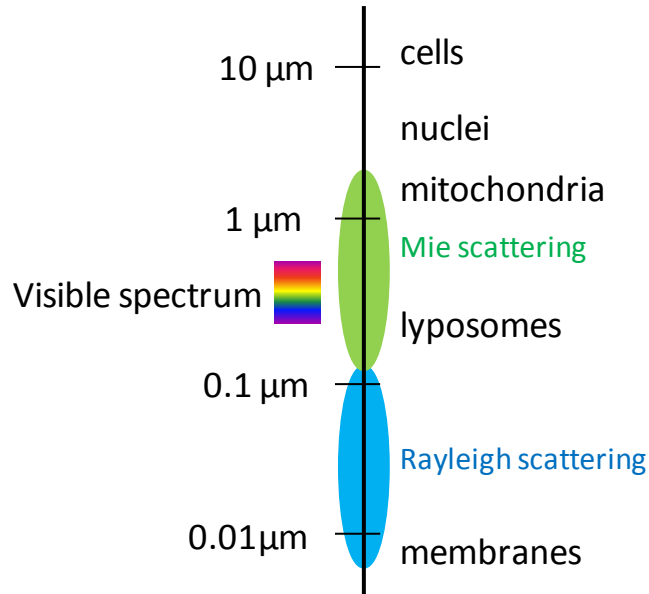


Figure 2.9: Scattering from typical cellular structures (as adapted from (Jacques SL, 1998(a))).

Scattering in tissue is generally caused by morphological variations in the tissue density and the refractive index (Welch A, 2011) (p46). Due to the scattering the light fluence rate ϕ [W/cm^2] just under the skin surface can be higher than the incident irradiance E_0 [W/cm^2] (Welch A, 2011) (p46). The increase in the fluence rate relative to the irradiance may in some cases be as high as a factor of five (Welch A, 2011).

Analogous to the absorption coefficient, the scattering coefficient (μ_s) can be defined as (Jacques SL, 1998(a)), (Dam JS, 2000(b)):

$$\mu_s = \rho_s \sigma_s \quad (2.8)$$

$[\text{cm}^{-1}] \quad [\text{cm}^{-3}] \quad [\text{cm}^2]$

with:

ρ_s = volume density of scatterers

σ_s = effective cross-sectional area of the scatterers

2.3.1.5 Anisotropy

The anisotropy, g , is a measure of the amount of forward direction retained by a photon after a single scattering event. When a photon is scattered by a particle so that its trajectory is deflected by a deflection angle θ , then the component of the new trajectory which is aligned in the forward direction is $\cos \theta$. The average deflection angle or the mean value of the cosine of the scattering angle, $\langle \cos \theta \rangle$, is defined as the anisotropy (Dam JS, 2000(b)). This is a dimensionless parameter that varies between -1 and 1 (backscatter to forward scatter). For

isotropic scattering, $g = 0$, there is a uniform distribution at all angles, but as g approaches 1, the distribution becomes highly peaked in the forward direction.

The Henyey-Greenstein model can be used to describe the angular distribution of light scattered by small particles. This model has been applied to numerous situations, ranging from the scattering of light by biological tissue to scattering by interstellar dust clouds (Henyey L, 1941). In this work the Henyey-Greenstein model is used to describe the angular distribution of light scattered from the subcellular particles in the skin:

$$\rho(\theta) = \frac{1}{4\pi} \frac{1 - g^2}{[1 + g^2 - 2g \cos \theta]^{3/2}} \quad (2.9)$$

2.3.1.6 Reduced scattering coefficient

In highly scattering media (e.g. skin) the photons propagate through the medium in consecutive steps which are random in length and direction (the so-called random walk). Each step commences with a scattering event that is equally likely to scatter the photon in any direction. The reduced scattering coefficient, μ'_s , describes isotropic scattering which is related to the (anisotropic) scattering coefficient, μ_s , through (Vo-Dinh T, 2003):

$$\mu'_s = (1 - g)\mu_s \quad (2.10)$$

For $g = 0.75$, an average of 4 scattering events is required for a population of photons to disperse isotropically. In tissue the value of g may vary from 0.4 to 0.99. This means that the photons are isotropically dispersed after anything from 2 to 100 scattering events (Vo-Dinh T, 2003) (p 2-25).

As noted in section 2.3.1.3, if a photon is detected at a specific point in or on the surface of the tissue, it is not possible to distinguish the path the photon took. In a medium with a specific reduced scattering coefficient, two photons may be detected at the same point after taking two completely different paths as illustrated in Figure 2.10 and Eq 2.11 (Dam JS, 2000(b)).

$$\mu'_s = (1 - g_1)\mu_{s1} = (1 - g_2)\mu_{s2} \quad (2.11)$$

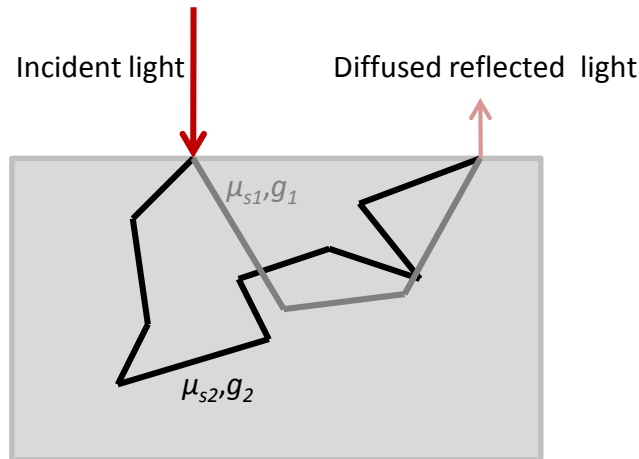


Figure 2.10: Similarity principle where photons taking different paths arrive at the same end point.

2.3.2 Values for the optical properties of skin

The optical properties of skin determine the fluence rate reaching deeper parts in the skin. During the past three decades, several researchers have measured the optical properties of different tissue types (Cheong WF, 1990), (Jacques SL, 1998(a)), (Simpson R, 1998(a)), (Salomatina E, 2006), (Tuchin V, 2007), (Tseng S, 2009). Comparing the published values for skin, it became apparent that the different authors did not report the same values for a variety of reasons. Table 2.3 is a summary of some of the published data for the optical properties of skin. Apart from the variance between different researchers, the optical properties of human skin also exhibit great variation between individuals and even from site to site on the body of the same patient (Zhang R, 2005).

Few references refer to the epidermal absorption coefficient for the different skin phototypes. There are some references (Zonios G, 2001), (Alaluf S, 2002(a)), (Alaluf S, 2002(b)), (Tseng S, 2009) but they mostly refer to a quantity known as the ‘melanin index’, for which the relation to the actual absorption coefficient is not particularly clear. Alaluf et.al. (Alaluf S, 2002(a)) reported on melanin concentration for the different skin phototypes (typically South African). Their findings were that the ‘African’ skin had about double the epidermal melanin concentration of the ‘European’ skin. This was true for both the sun-exposed and non-exposed skin samples retrieved from 4 mm punch biopsies. It is not a straight forward process to convert the melanin concentrations measured from the skin biopsies to the corresponding absorption coefficients. It is also reported that for the darker skin phototypes the melanin particle sizes are usually larger than for the lighter skin phototypes (Alaluf S, 2002(a)).

Table 2.3: Comparison of optical properties measured in various laboratories. Note: most authors publish the data in units of cm^{-1} and therefore this table uses cm^{-1} but in the rest of this work units of mm^{-1} are used (Table adapted from (Tuchin V, 2007)).

Tissue	λ (nm)	μ_a (cm^{-1})	μ_s (cm^{-1})	μ'_s (cm^{-1})	g	Reference
Epidermis	600	19	460	-	0.80	(van Gemert MJC, 1989)
Epidermis	633	35	450	88	0.80	(van Gemert MJC, 1989)
Epidermis	633	2.6	-	47.6	0.80	(Salomatina E, 2006)
Epidermis (caucasian)	633	0.35	-	27.5	-	(Simpson R, 1998(a))
Epidermis (negroid)	633	2.6	-	32.5	-	(Simpson R, 1998(a))
Epidermis (type I-II)	633	0.63	-	22.4	-	(Tseng S, 2009)
Epidermis (type III-IV)	633	0.66	-	22.3	-	(Tseng S, 2009)
Epidermis (type V-VI)	633	0.73	-	22.1	-	(Tseng S, 2009)
Epidermis	800	40	420	62	0.85	(van Gemert MJC, 1989)
Epidermis	820	1.5	-	36	0.80	(Salomatina E, 2006)
Dermis	600	2.2	200	-	0.80	(van Gemert MJC, 1989)
Dermis	633	2.7	187.5	37	0.80	(van Gemert MJC, 1989)
Dermis	633	1.9	-	23.8	-	(Tuchin V, 2007)
Dermis	633	<10	-	11.64	0.97	(Tuchin V, 2007)
Dermis	633	1.5	-	50.2	-	(Tuchin V, 2007)
Dermis	633	1.5	-	29.9	0.80	(Salomatina E, 2006)
Dermis	800	2.3	175	30	0.85	(van Gemert MJC, 1989)
Dermis	820	1.1	-	21.8	0.80	(Salomatina E, 2006)
Skin (negroid)	633	2.41	-	32.2	-	(Simpson R, 1998(b))
Skin (caucasian)	633	0.33	-	27.3	-	(Simpson R, 1998(b))

Skin damage (including blistering) has been reported during laser hair removal procedures on darker skin phototypes (Lanigan S, 2003), (Battle E, 2004). This underlines the importance of determining the absorption coefficient of the skin before laser treatment commences.

It is important to note that there are differences in optical properties depending on whether the measurements were done *in vivo* or *in vitro*. In general *in vivo* measured values of μ'_s and μ_s are two to ten times smaller than *in vitro* measured values (Tuchin V, 2000) (p37).

The wide range in reported μ_a values for the epidermis made it difficult to extract the required μ_a values from the published literature. This work is aimed at the *applicability of laser based treatment to the South African population*. The lack of consistency in reported μ_a values prompted the author to investigate techniques that can be used to determine the optical properties of tissue, specifically the epidermis, non-invasively. This will be discussed in the next section.

2.4 MEASUREMENT TECHNIQUES

To the knowledge of the author, there is no established technique that can be used to directly measure the optical properties of tissue. All the techniques rely on inverse methods to determine the optical properties. The two methods used in this work are an integrating sphere (IS) and a diffuse reflectance probe (DRP). In both methods, the optical properties are calculated from the average properties in the sampled (illuminated) area. These average values are later used in the computer model that requires an average value of the optical properties for each layer.

2.4.1 Integrating sphere

An integrating sphere (IS) can be described as a hollow sphere with a few ports (entrance, exit and detector). The inside of the sphere is coated with a highly reflective material. In the visible and near infrared wavelength regions (400-1500 nm), the coating is usually Spectralon with a reflectivity of more than 98% (Labsphere, 2012). An IS system integrates the radiant flux spatially and can be used to measure optical radiation (Labsphere, 2012).

IS systems are widely used to measure the optical properties of various materials, including human tissue (Pickering JW, 1993), (Nilsson AM, 1998), (Dam JS, 2000(b)), (Bashkatov AN, 2005), (Salomatina E, 2006), (Singh A, 2009), (Singh A, 2011). This method uses one or two Integrating Spheres to measure the reflectance from a sample and the transmission through the sample as shown in Figure 2.11. For these measurements, the underlying assumption is that the sample is homogeneous.

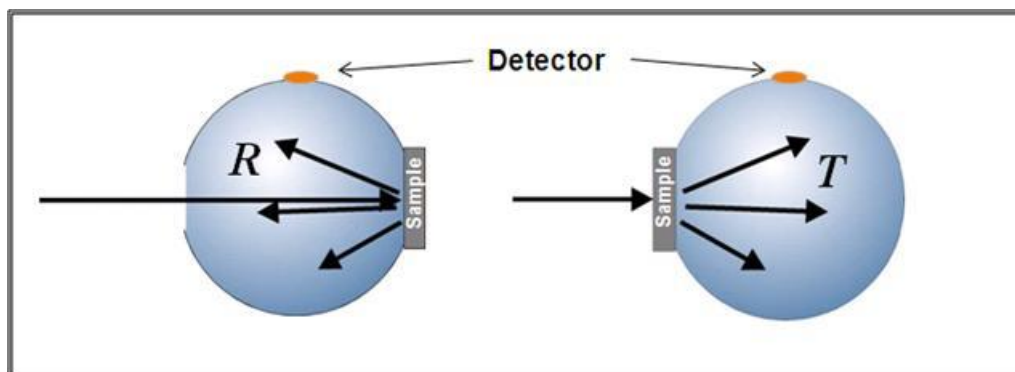


Figure 2.11: Integrating sphere system for reflection (R) and transmission (T) measurements.

For a single sphere the sample is moved from the port closest to the light source to the opposite port to measure either the transmitted or reflected light. The light beam for the IS is usually about 2-4 mm in diameter. For the efficient use of the IS, samples need to have a

diameter of > 15 mm. This means that the same area is not necessarily sampled during the measurements when the samples are moved from the one port to the other.

In a double IS system, two spheres are put next to each other with only the sample holder between the two spheres. In this configuration the same area is sampled for both the transmission and reflection measurements. In the double IS system cross-talk between the spheres may influence the data (Nilsson AM, 1998), (Dam JS, 2000(b)), (Salomatina E, 2006).

The IS system needs to be calibrated with a set of phantoms with known absorption and scattering coefficients. The optical properties of the sample under investigation are then determined from the measurements using the calibration model to extract the values using a multiple polynomial regression method (Dam JS, 2000(a)), (Dam JS, 2000(b)). The method involves fitting different order polynomial functions of μ_a and μ'_s to the measured data and then predicting μ_a and μ'_s for the particular sample using a Newton-Raphson algorithm.

The IS system is not suitable to measure optical properties of skin *in vivo*. In order to use the IS system to measure the optical properties of skin, samples must be acquired either through skin biopsies or excess skin from surgical procedures. This is an invasive process. A less invasive measurement technique using diffuse reflectance is discussed in the following section.

2.4.2 Diffuse reflectance probe

In the recent decade numerous papers have been published where the optical properties of skin were measured, non-invasively, with a diffuse reflectance probe (Dam JS, 2000(b)), (Johns M, 2005), (Zonios G, 2006), (Reif R, 2007), (González FJ, 2010). Light entering skin can be scattered directly from the surface of the skin and a portion of the light may enter the skin and be reflected/scattered from deeper lying structures as indicated in Figure 2.12. It is this diffusely reflected light that is detected with a diffuse reflectance probe (DRP). A typical layout for a DRP experiment is shown in Figure 2.13.

The scattered light that exits the skin sample can be collected by a detector placed some distance from the light source. By measuring the diffusely reflected light as a function of wavelength (usually with a spectrometer) the values of μ_a and μ'_s can be calculated. Some systems use a probe with a single detection fibre and a single or multiple emitting fibres (Johns M, 2005), (Zonios G, 2006), (Reif R, 2008) while others use multiple detection fibres which are placed at different distances from the source (Dam JS, 2000(b)), (Meglinski IV, 2002), (Wang Q, 2008). Using different distances between the light emitting fibre and the

detecting fibres allow the user to probe different depths into the skin because the further the distance between the emitting and collection fibres, the ‘deeper’ the light can travel into the skin and still be detected by the collecting fibre (Meglinsky IV, 2001), (Doronin A, 2011). The probe system used in this work had a fixed light delivery-detector distance and only the outer layers of the skin could be sampled.

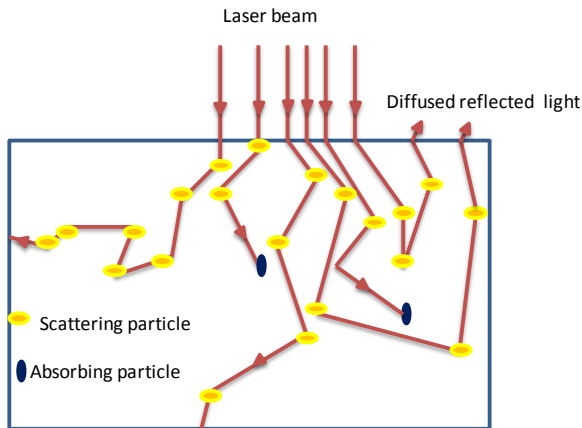


Figure 2.12: Absorption and scattering in skin.

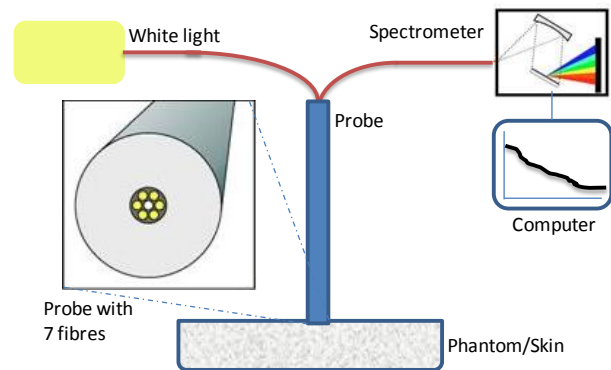


Figure 2.13: Schematics of an experimental setup for the diffuse reflectance probe measurements.

2.5 SKIN SIMULATING PHANTOMS

Due to the difficulties in handling human tissue, phantoms are used to simulate the properties of tissue/skin. Over the years skin simulating phantoms have been developed in order to test and calibrate bio-optical instrumentation and techniques. Skin simulating phantoms can be broadly divided into three categories: liquid, gel and solid phantoms (Pogue B W, 2006). Liquid phantoms, usually prepared from biological materials e.g. intralipid (IL), have the advantage that they are easy and quick to prepare but do not usually have a long shelf life. They are usually used to calibrate systems e.g. IS or reflectance probe systems, but are not used as long term reference standards. Gel based phantoms provide more flexibility, but also have a limited shelf life and must be stored correctly, usually in a liquid, which in itself has an effect on the measured optical properties. Solid phantoms are generally more cumbersome to prepare, but are stable over longer periods of time and can be used as a calibration standard for systems. Phantoms usually consist of a host material (or matrix) with both absorbers and scatterers added to the matrix. In this work only liquid and solid phantoms were used. Both liquid and solid phantoms were used to validate the computer model discussed in Chapter 3.

When scattering and absorbing particles are used in phantoms to mimic skin behaviour, it is assumed that the scattering particles do not absorb light at the investigating wavelength (assume $\mu_a = 0$). Similarly it is assumed that the absorbing particles do not scatter the light.

2.5.1 Liquid phantoms

Intralipid (IL) is a known simulant for scattering in human skin. It is a white, fat based emulsion with spherical particles (mean diameter of 0.4 μm) (Das BB, 1997). It is usually supplied in a concentration of 20% volume IL/total volume in a mixture consisting of the IL and distilled water. The IL is mixed with an equal volume of an absorbing mixture consisting of distilled water and absorbing particles (black ink or carbon black particles). The optical properties of IL (diluted to a concentration of 10% IL in distilled water) are well documented for HeNe lasers ($\lambda = 632.8 \text{ nm}$) (van Staveren HJ, 1991), (Flock S, 1992), (Michielsen K, 1998), (Choukeife JE, 1999). At this wavelength μ'_s and μ_a for IL is given by (van Staveren HJ, 1991):

$$\mu'_{s(\lambda=632.8 \text{ nm})} = 1.104 \text{ mm}^{-1} \times (\text{IL concentration}) \quad (2.12)$$

and

$$\mu_{a(\lambda=632.8 \text{ nm})} = 0.15 \times 10^{-2} \text{ mm}^{-1} \times (\text{IL concentration}) \quad (2.13)$$

The value of μ_a for IL is about 10^3 smaller than μ'_s and is generally disregarded for the 10% IL. The anisotropy can be calculated by (van Staveren HJ, 1991):

$$g = 1.1 - 0.58\lambda \quad (2.14)$$

with λ between 0.4 and 1.1 μm (with the units of λ in μm).

To calculate the μ_a of the ink sample, the intensity of the laser (I_0) without the ink and with the ink (I) is measured as well as the path length (d) though the sample (cuvette). The Beer-Lambert law discussed in section 2.3.1.3 is then used to calculate the μ_a at the required wavelength.

$$\mu_a = \frac{1}{d} \ln \frac{I_0}{I} \quad (2.15)$$

2.5.2 Solid phantoms

Solid phantoms are usually prepared by using a resin (with a high transmission and low absorbance at the required wavelength) as base material (or matrix) with added scatterers (TiO) and absorbing particles (carbon black). The optical properties of the solid phantoms are determined by the concentration of the TiO and carbon black added to the matrix.

2.6 LIGHT PROPAGATION MODELS

A continuing increase in medical applications of lasers both for treatment and diagnostic purposes (Peng Q, 2008), (Overton G, 2011) necessitates the ability to model the laser-tissue interaction mechanisms. The purpose of computer model simulations is to predict the fluence rate as a function of depth inside the tissue (Cheong WF, 1990). The accuracy of these predictions is dependent on how well the model simulates the tissue and the validity of the values of the optical properties used in the model.

The focus of this work is on the implementation of a computer model developed in a commercially available software environment and therefore only a brief overview is given of the major models predicting light propagation through tissue. More extensive formulations can be found in (Splinter R, 2007), (Martelli F, 2010), (Welch A, 2011).

A fundamental theory of light propagation in multiple scattering media has been developed by applying Maxwell's equations (Dam JS, 2000(b)), (Martelli F, 2010). This theory preserves the wave properties of the light and is able to account for all the effects of multiple scattering, diffraction and interference. The complexity of this rigorous mathematical formalism is overwhelming and even with fast computers and computing techniques no practical models for general use in multi-scattering media is available as yet (Cheong WF, 1990), (Dam JS, 2000(b)), (Martelli F, 2010) .

For practical applications one has to resort to numerical models based on the solution of the radiative transport equation. (Dam JS, 2000(b)).

2.6.1 Radiative Transport equation

The radiative transport equation (RTE) describes the transport of energy through a scattering medium phenomenologically (Ishimaru A, 1989), (Martelli F, 2010). In the electromagnetic theory (Maxwell's equations) the propagation of light is described by the superposition of electromagnetic fields while the transport theory depends on the superposition of energy fluxes (Dam JS, 2000(b)), (Jacques S, 2008(b)). Even though the radiative transport theory lacks the rigorous mathematical formulation of the Maxwell's equation approach, it is able to account for all the physical effects involved in light propagation (Martelli F, 2010).

Multiple scattering is associated with de-coherence of the light and therefore in turbid media the wave nature of light is suppressed (Vo-Dinh T, 2003). Most of the laser-tissue interaction models are based on the RTE (Cheong WF, 1990), (Jacques SL, 1998(b)). The

RTE does not have exact closed form analytical solutions which are relevant in most practical applications.

Two of the most common methods used to solve the RTE are the diffusion approximation and the Monte Carlo simulation (or probabilistic) method.

2.6.1.1 Diffusion approximation

This approximation provides useful solutions when certain restrictions are taken into account. In the diffusion theory, the photon migration is modelled as a gradient-driven diffusion of energy or energy flux (Dam JS, 2000(b)), (Jacques S, 2008(b)). A restriction in the diffusion approximation is that a photon must undergo several scattering events before it is absorbed.

In the diffusion approximation it is assumed that the radiant energy does not travel in a preferential direction. When a laser or collimated beam is directed onto skin, the photons have a specific direction of movement (Mustafa FH, 2011). During the scattering process in the skin, they lose their directionality and the diffusion approximation can be implemented (Jacques S, 2008(b)). One of the assumptions of the diffusion theory is that the photons take part in a random walk. For this to happen, a photon must undergo several scattering events before it is absorbed. The commonly cited rule of thumb is that $\mu'_s/\mu_a > 10$ (Star WM, 1988), (Dam JS, 2000(b)), (Jacques S, 2008(b)), (Martelli F, 2010). With enough scattering events, the average photon propagation depends on the product $(\mu_s(1 - g))$ rather than on the specific values of μ_s and g (Star WM, 1988), (Jacques S, 2008(b)).

For modelling light transport in skin and especially the epidermis with high absorption coefficients, the diffusion approximation condition ($\mu'_s/\mu_a > 10$) is not always met. The Monte Carlo process is an alternative light transport model used in the skin when the diffusion approximation assumption is too stringent.

2.6.1.2 Monte Carlo simulations

Monte Carlo (MC) simulations can be used as an alternative modelling technique to solve the radiative transport equation (Vo-Dinh T, 2003), (Martelli F, 2010), (Welch A, 2011). It is a stochastic or randomised approach. In this method the trajectories of photons are traced through the model, making use of the particle nature of the photons. MC methods are used to simulate the photon path of a great number of photons (more than 1 million). The path of each photon is traced as it undergoes scattering and absorption. It is a purely stochastic approach and models light as discrete photons bouncing around in the scattering medium

(Dam JS, 2000(b)). The assumption is also made that the media are homogeneous. MC simulations are not constrained by the condition that the absorption coefficient should be smaller than the reduced scattering coefficient (diffusion approximation). The only requirement is to define the turbid medium using its scattering and absorption coefficients as well as the anisotropy (Private communication with Breault Research, vendor of the ASAP software).

The Monte Carlo process

The MC process consists of a number of steps

- MC process is a statistical process and therefore a large number of photons are launched into the medium (typically more than 1 million). The effect of a few photons compared to that of 3.1 million photons is illustrated in Figures 2.14 and 2.15.

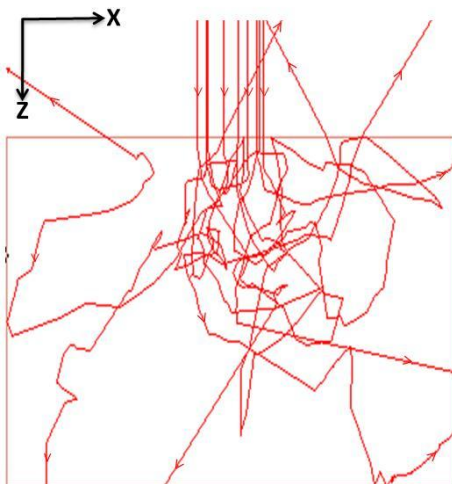


Figure 2.14: Random walk of 15 photons.

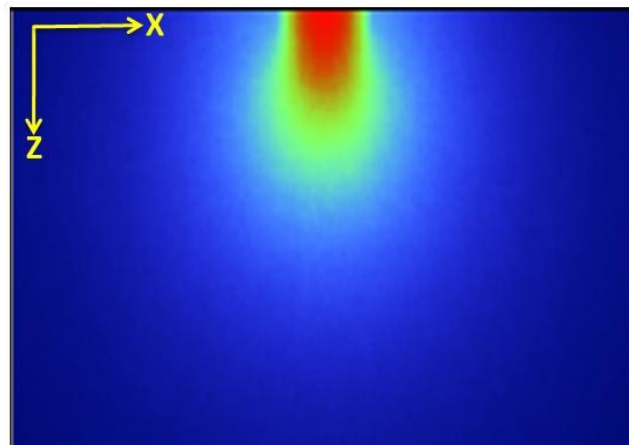


Figure 2.15: Random walk of 3.1 million photons.

- Each photon performs a random walk in the skin. The path of a photon is decided by a number of iterative decisions along the path of the photon:
 - The distance a photon travels before an interaction occurs.
 - The direction in which the photon proceeds after the interaction.
- The macroscopic optical properties, μ_a and μ_s , determine the path length of a photon between interactions and the anisotropy, g , determines the direction of travel in the random process.
- The step size or path length of a photon between photon-tissue interaction sites is given by

$$l = \frac{-\ln(\xi)}{(\mu_a + \mu_s)} \quad (2.16)$$

with ξ a uniformly distributed random number between 0 and 1.

- A photon ‘loses’ part of its energy after each step by an amount of (1- albedo), where

$$albedo = \frac{\mu_s}{(\mu_a + \mu_s)} \quad (2.17)$$

2.6.2 Raytracing models

In this work the Monte Carlo approach was used because the radiative transport equation requirement, $\mu'_s/\mu_a > 10$, is too stringent when applied to visible light interaction with the epidermal layer.

Raytracing has been used for many decades to design optical systems (Stevenson M, 2006). Free software is available online (e.g MCML – Monte-Carlo Modelling of Light transport (Jacques SL, 1998(b))), or commercially (e.g. ASAP from Breault Research Organization). The online software assumes symmetry around the light source (Jacques SL, 1998(b)), but this is not always desirable.

The ASAP (Advanced Systems Analysis Program) software from Breault Research Organization (Tucson, Arizona in the USA) is capable of performing non-sequential raytracing where rays (or photons) can interact with objects as they are encountered. The rays are not restricted to the order in which the objects were defined in the model as is the case in sequential raytracing (Michel B, 2005), (Breault Research, 2006). ASAP does not assume symmetry and allows for any geometrical shape to be used.

The following were taken into account on the decision to use ASAP:

Advantages of ASAP:

- Any shape of form can be modeled, irregular shapes can be used and predefined or measured shapes can be imported through computer aided design (CAD) software. Some tumors may have irregular shapes.
- Geometrical changes are relatively easy to implement.
- The system is a raytracing software package and as such in is applicable for more than just laser tissue interaction modeling.

Disadvantages of ASAP:

- The software is expensive.
- It has not been widely applied in peer-reviewed articles.

The verified model developed in the ASAP environment is described in more detail in Chapter 3. The model was applied to a cancer therapy which is described in the next section.

2.7 CANCER AND PHOTODYNAMIC THERAPY

According to the latest statistics available from the Cancer Association of South Africa (CANSA), non-melanoma skin cancer (consisting of basal cell carcinoma (BCC) and squamous cell carcinoma (SCC)) is the most common type of cancer in South Africa with about 20 000 new cases reported each year. Australia and South Africa have the highest incidence of skin cancer in the world (Mqoqi N, 2004).

“Basal cell carcinoma accounts for more than 90% of all skin cancers. Basal cell cancer grows slowly and does not usually spread to other parts of the body. However, if left untreated, it can spread to nearby areas and invade bone and other tissues under the skin. Squamous cell carcinoma (SCC) is much less common than BCC but can be more aggressive than BCC and is also more likely to grow deep below the skin and spread to distant parts of the body. When squamous or basal cell skin cancers are found early, there is nearly a 100 % chance for cure” (MD Anderson Cancer Centre, 2009). Both BCC and SCC may potentially be treated with photodynamic therapy.

2.7.1 Photodynamic therapy (PDT)

Photodynamic therapy (PDT) is one of the newer cancer treatments under investigation worldwide (Schuitmaker J, 1996), (Hopper C, 2000), (Brown SB, 2004), (Robertson CA, 2009), (Sekkat N, 2012). PDT is usually defined as the administration of a non-toxic drug or dye (sometimes called photosensitiser (PS)) either systemically, locally or topically to the patient with a tumour. After some delay allowing for the PS to accumulate in the tumour, the tumour is irradiated with light where the wavelength has been tuned to an absorption peak of the PS. In the presence of oxygen toxic species are formed that lead to cell death and tissue destruction in the tumour. The PS preferentially accumulates in tumour cells rather than normal cells. One of the major features of PDT as a treatment modality is its dual selectivity, both light and the PS must be present for the destruction of the cells. Collateral damage to normal tissue can be minimised by delivering the light only to the affected area that requires treatment. Tumours can be destroyed rapidly and any damage to healthy tissue usually heals within a few weeks (Brown SB, 2004).

The more recent use of PDT in oncology dates back to the early 1970's when Dr. Thomas J. Dougherty started his investigations into the mechanisms and clinical use of

hematoporphyrin derivatives (HpD). Since then PDT has been approved in numerous countries (Mang TS, 2004). A list of some of the photosensitisers (PS's) and their potential therapeutic applications can be found in (Sekkat N, 2012).

2.7.1.1 Photodynamic interaction mechanism

“Light absorption and energy transfer is at the heart of PDT. The ground state PS has two electrons with opposite spins in the low energy molecular orbital. After the absorption of photons, one of these electrons is excited to a high energy orbital, but keeps its spin (first excited singlet state)” (Castano AP, 2004). The electron stays in this excited state for only a few nanoseconds before losing its energy through fluorescence, internal heat conversion or intersystem crossings as illustrated in Figure 2.16 (Castano AP, 2004), (Zhu TC, 2006). The fluorescence has some added benefits as it can be used to quantify the amount of PS in the cells or tissue or as *in vivo* fluorescence imaging to follow the distribution of the PS.

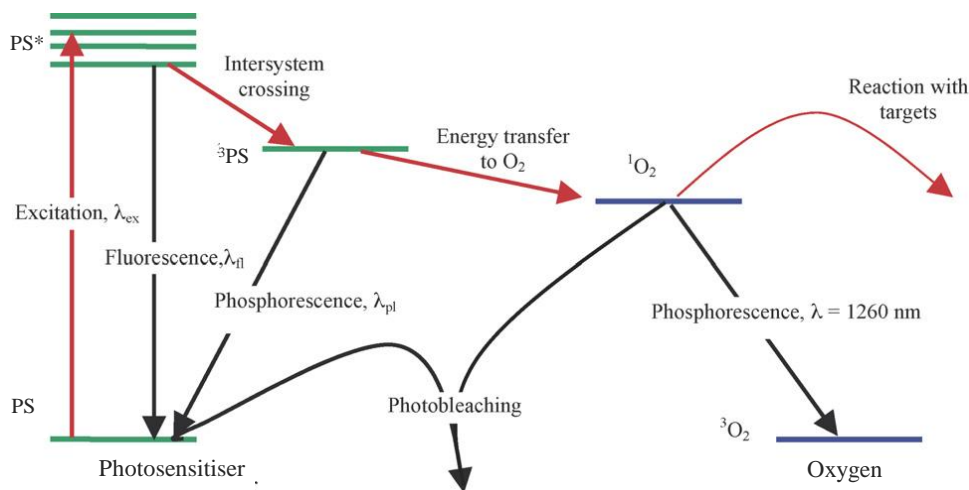


Figure 2.16: Energy level diagram for a Type 2 photosensitiser.

A relatively long-lived (in the order of microseconds) excited triplet state is formed during the intersystem crossing. From the excited triplet state the PS can follow two paths or reactions to induce cell death. (Castano AP, 2004), (Zhu TC, 2006) (p235 – 236).

- Type 1 reaction:
 - Direct interaction with a cell membrane or a molecule. This interaction may generate cytotoxic free radicals.
 - Further reactions of the free radicals with oxygen may produce reactive oxygen species.

- Type 2 reaction:
 - In this reaction, excited state singlet oxygen is formed directly by the transfer of energy from the PS in the triplet state.

It is possible for both type 1 and 2 reactions to occur simultaneously. In this case the ratio between the two processes depends on various factors (i.e. the type of PS used, the concentration of the PS in the tissue and the oxygen levels in the tissue). The majority of the newer PS compounds available for PDT utilise the Type 2 process (Zhu TC, 2006). The energy levels in Figure 2.16 explain some of the underlying physical processes during in a Type 2 PDT process. Highly reactive singlet oxygen ($^1\text{O}_2$) is formed and the PS returns to its ground state. During this process the PS is not ‘consumed’ and can create another singlet oxygen molecule.

Singlet oxygen has a short half-life and is highly reactive. Therefore only molecules and structures that are close to the PS are directly affected by PDT (Castano AP, 2004). In cells the typical half-life of singlet oxygen is less than 40 ns. The singlet oxygen is only active in a radius of the order of 20 nm (Castano AP, 2004).

An effective PDT process is dependent on the absorption of light by the PS. As such it is important to ensure that the required fluence rate reach the PS in the tumour. The term light dose or treatment dose (J/cm^2) is often used in PDT treatment. When a continuous wave laser is used, this dose term will combine the fluence rate and treatment time (energy = power \times treatment time).

Optical properties of tissue, and particularly in skin, are important in laser applications such as PDT and biostimulation. Epidermal absorption of the light reduces the fluence rate reaching the intended treatment site. The layered structure of skin, combined with the optical properties of the different layers, can be used in a computer model to predict the laser fluence rate at the treatment site.

2.8 SYNTHESIS

The absorption of light in the epidermal layer of the skin is a factor that is not usually considered during laser skin treatments. Epidermal absorption is dependent on the skin phototype and if not taken into account, may result in unwanted skin damage (Lanigan S, 2003), (Lepselter J, 2004), (Lim SRP, 2006).

With the information discussed in this chapter, it has become apparent that a computer model may be a useful tool to predict the fluence rate at any depth into the skin. Depending

on the skin site, there may be a large variation in the absorption of light in the epidermal layer of the skin. This influences the transmission of light through the epidermis and as a result influences the fluence rate available for treatment deeper into the skin. A predictive computer model may enable a clinician to adapt the treatment parameters to the specific treatment site at the required depth of treatment for the patient.

Computer models that can trace light through tissue do exist (Jacques SL, 1998(b)), (Breault Research, 2006). Modifying software developed by other authors to accommodate one's own specific application requirements is not always practical. Investigation into existing software led to the decision to acquire the commercially available ASAP software package from Breault Research Inc. While their Realistic Skin Model (RSM) is a useful tool, it is too complex to be validated with skin simulating phantoms that can be prepared in a research laboratory where a simpler model is required to test the influence of specific parameters on the fluence rate at a specific depth into the skin. The major influencing factors under investigation are the epidermal absorption (absorption coefficient for the individual to be treated) and the thickness of the epidermal layer (body site to be treated). The development of such a simpler model in the ASAP environment and the experimental validation is discussed in the next chapter (Chapter 3).

The second 'stumbling block' in the prediction of the fluence rate in the skin is the lack of data on the absorption coefficient for the different skin phototypes (see section 2.3.2). Due to the importance of this parameter for the computer model, the absorption coefficient had to be measured on a sample that is representative of the South African population. The most appropriate non-invasive technique that could be identified was the diffuse reflectance probe (DRP) technique described by Zonios (Zonios G, 2006). The development of this technique, the accompanying software as well as the *in vivo* test on 30 volunteers is described in Chapter 4. This DRP technique is a fast, cost effective, non-invasive and portable technique that has the potential to be implemented at "point-of-care" in South Africa.

The final implementation of the computer model for different skin phototypes as well as different epidermal thicknesses is discussed in Chapter 5.

The discussion in this review chapter led to the following conclusions that are important for this work:

- The optical properties influence light transmission through skin and as such the fluence rate reaching deeper into the skin.

- Basic optical ray tracing models are not sufficient due to the multi-scattering in tissue.
- Layered structured computer models are available commercially and online.
- The online software (MCML, (Jacques SL, 1998(b))) is cumbersome to use and geometry changes are not easy to implement.
- Change in geometry is important in a fluence rate prediction model. The ASAP software allows for this.
- Both models (ASAP and MCML) are based on the Monte Carlo simulation process where vast numbers of photons are traced through the model.
- Data on the expected range of absorption coefficients for the South African population is not available. Data is scarce for the absorption coefficient of the different skin phototypes. For the implementation of the model in the South African environment, this data is necessary.

This led to the conclusions that:

- A computer model (with flexibility to add structures in the model, e.g. tumours) must be developed to predict the fluence rate at any pre-determined depth into skin.
- The extent of the epidermal absorption coefficient spread for the South African skin phototypes needs to be measured. A diffuse reflectance probe provides the capability to do that.
- The influence of the epidermal absorption influences the fluence rate that is available for treatment some distance into the skin. This needs to be quantified for the South African population.

In the next chapters the development of the computer model is discussed as well as the development of a diffuse reflectance probe measurement protocol and data extraction with the introduction of representative absorption coefficients into the computer model. The computer model is then used to give an indication of the treatment time adjustments required for different skin phototypes present in the South African population.

The next chapter will be devoted to the development, verification and validation of the layered structure computer model to simulate skin.